Appl Phys B (2008) 92: 577–583
DOI 10.1007/s00340-008-3106-3

Applied Physics B
Lasers and Optics

Multi-layer cladding leaky planar waveguide for high-power applications

A. Kumar · V. Rastogi

Received: 1 March 2008 / Revised version: 11 June 2008 / Published online: 2 August 2008

Abstract We design a multi-layer cladding large-core planar waveguide that supports a single guided mode. The waveguide works on the principle of higher-order mode discrimination. The cladding of the waveguide is formed by alternate low- and high- index regions, which helps leaking out of higher-order modes while retaining the fundamental mode over the entire length of the waveguide. The structure is analyzed by the transfer-matrix method and the leakage losses of the modes have been calculated. We show that a waveguide formed in silica with numerical aperture 0.24 and core width 10 μm can be designed to exhibit single-mode operation at 1550-nm wavelength. Such a structure should find applications in high-power planar waveguide lasers and amplifiers.

PACS 42.82.-m · 42.82.Et · 42.79.Gn · 42.55.-f · 42.82.Bq

1 Introduction

Planar waveguide lasers (PWLs) are attractive for making compact laser systems using high power diode array pumping and for the possibility of aligning various optical components on a single substrate [1–7]. Another benefit of the planar geometry is the high degree of thermal immunity due to its large cooling-surface-area-to-volume ratio, which is helpful in controlling the active layer temperature in high average power devices [1, 2]. Waveguide lasers and amplifiers preferably require the structures that support a single guided mode to avoid inter-modal competition and to have good beam quality. However, in a conventional optical waveguide, a thin core, needed for single-mode (SM) operation, increases the power density inside the core and, thus, limits the power-handling capacity of the waveguide. The high power density in the core can also give rise to undesired nonlinear effects and can lead to instability in the operation of the laser by mixing signal and pump wavelengths. In view of this, there is significant interest to design large-core-area SM waveguides. In fiber geometry, considerable efforts have been made to enhance the power-handling capacity by employing large-mode-area (LMA) designs [8–20]. Some of the designs include lowering the numerical aperture (NA) and tailoring the refractive-index profile in rare-earth-doped fibers [8–11]. Another way to achieve the high power fiber laser is to use a suitable cladding pumping scheme [12–14]. Use of photonic crystal fibers (PCFs) which are characterized by a distribution of air holes in the cladding running through the entire length of the fiber is another way of achieving LMA operation [15]. Recently, some schemes based on higher-order-mode discrimination have been proposed for LMA fibers. In these designs the cladding refractive-index profile has been tailored in radial or angular directions to strip off higher-order modes and achieve SM operation with large mode area [16–20].

Recently, we proposed a graded-index cladding design in planar geometry [21] and a geometrically shaped leaky cladding in channel waveguide [22] to have a large-core SM waveguide that works on the principle of higher-mode discrimination. The planar waveguide structure proposed in Ref. [21] has a graded-index cladding and can exhibit SM operation with a 10-μm core and 0.17 NA. In this paper, we propose another leaky design, which, in contrast to our previous graded cladding, consists of multi-layer cladding and should be easier to fabricate. The cladding of the proposed

A. Kumar · V. Rastogi (✉)
Department of Physics, Indian Institute of Technology Roorkee, Roorkee 247 667, India
e-mail: vipul.rastogi@osamember.org
Fax: +91-1332-273560

structure is formed by alternate low- and high-index regions. All the high-index regions have the same refractive index as that of the core, while the depressed (low-index) cladding regions follow a power-law variation. The structure has been analyzed by the transfer-matrix method (TMM) to calculate the effective indices and the leakage losses of the first two modes [23, 24]. A large differential leakage loss between the fundamental and the higher-order modes with a tolerable loss for the fundamental mode ensures effective SM operation of the waveguide. We show that a waveguide with core thickness 10 μm and 0.24 NA can effectively behave as a SM waveguide in the optical communication window. Such high-NA waveguides are preferred in planar geometry in order to have efficient pumping using diode-bar lasers and to have high bending tolerance [6, 25]. A conventional waveguide with such core size and index contrast would have supported three modes. The proposed design should be useful for high power planar waveguide lasers and amplifiers.

2 Waveguide structure and method of analysis

The proposed structure consists of a uniform substrate, a uniform guiding core, and a multi-layer cladding, as shown in Fig. 1. The core of width a has the refractive index n_1, while the cladding of width $b-a$ is formed by alternate low- and high-index regions. The high-index cladding regions have the same refractive index as that of the core and the refractive index of the depressed region is subjected to power-law variation given by

$$n^2(x) = n_1^2\left(1 - 2\Delta\left(\frac{b-x}{b-a}\right)^q\right), \quad a < x < b, \tag{1}$$

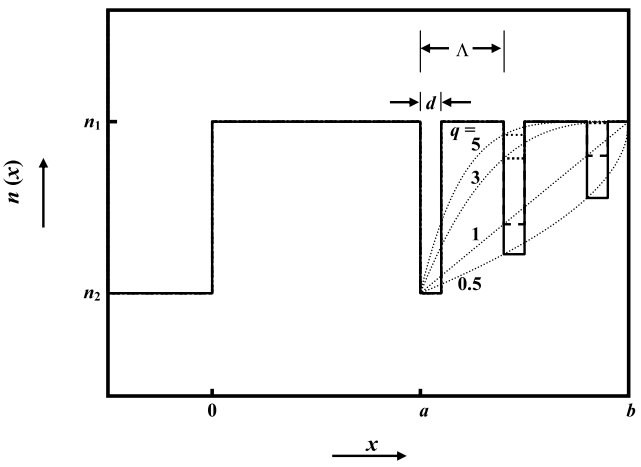

Fig. 1 Refractive-index profile of multi-layer planar waveguide for three different values of profile parameter q

where q (>0) is called the profile shape parameter. $\Delta = \frac{n_1^2 - n_2^2}{2n_1^2}$ is the relative index difference between the guiding core and the first cladding layer, n_2 being the refractive index of the first depressed layer of the cladding. The NA of the waveguide can, thus, be defined as $n_1\sqrt{2\Delta}$. d represents the width of the depressed cladding layer while the periodicity of the low- and high-index cladding layers is defined by Λ. The high-index layers in the cladding make the structure leaky and the SM behavior of the waveguide can be ensured by a high differential leakage loss between the first two modes. The structure can be analyzed by using the TMM to calculate the effective indices and the leakage losses of the modes [23, 24]. To implement the TMM in a multi-layer waveguide, one can write the electric field in the ith layer of width d_i and refractive index n_i as

$$E_i = \begin{cases} A_i \cos[k_i(x - d_{i+1})] + B_i \sin[k_i(x - d_{i+1})], \\ \quad \kappa_i^2 > 0, \\ A_i \cosh[k_i(x - d_{i+1})] + B_i \sinh[k_i(x - d_{i+1})], \\ \quad \kappa_i^2 < 0, \end{cases} \tag{2}$$

where $k_i = |\kappa_i|$, $\kappa_i^2 = k_0^2(n_i^2 - n_{\text{eff}}^2)$, $k_0 = 2\pi/\lambda$ is the free-space wavenumber, and $n_{\text{eff}} = \beta/k_0$ is the effective index of the mode with β being the propagation constant. By applying suitable boundary conditions at the interface between the ith and $(i+1)$th layers, the field coefficients, A_i, B_i, A_{i+1}, and B_{i+1}, can be related by a 2×2 matrix:

$$\begin{pmatrix} A_{i+1} \\ B_{i+1} \end{pmatrix} = S_i \begin{pmatrix} A_i \\ B_i \end{pmatrix}, \tag{3}$$

where S_i is known as the transfer matrix of the ith layer. For the TE mode, S_i is given by

$$S_i = \begin{pmatrix} \cos\Delta_{i+1} & -(\frac{k_i}{k_{i+1}})\sin\Delta_{i+1} \\ \sin\Delta_{i+1} & (\frac{k_i}{k_{i+1}})\cos\Delta_{i+1} \end{pmatrix}, \quad \text{for } \kappa_i^2 > 0,$$
$$= \begin{pmatrix} \cosh\Delta_{i+1} & (\frac{k_i}{k_{i+1}})\sinh\Delta_{i+1} \\ \sinh\Delta_{i+1} & (\frac{k_i}{k_{i+1}})\cosh\Delta_{i+1} \end{pmatrix}, \quad \text{for } \kappa_i^2 < 0, \tag{4}$$

where $\Delta_i = k_i(d_i - d_{i+1})$. The field coefficients of the first and the last layers of the structure can then be related by multiplying the transfer matrices of all the intermediate layers:

$$\begin{pmatrix} A_N \\ B_N \end{pmatrix} = f \begin{pmatrix} A_1 \\ B_1 \end{pmatrix}, \tag{5}$$

where $f = S_{N-1}S_{N-2}\cdots S_1$ with

$$f = \begin{pmatrix} f_{11} & f_{12} \\ f_{21} & f_{22} \end{pmatrix}. \tag{6}$$

For a leaky waveguide, in the high-index outermost region only the outgoing wave exists and in the low-index substrate

region no amplifying term is allowed. These conditions lead to $A_1 = \mathrm{i}B_1$ and $A_N = -B_N$. From (5) and (6), we can write

$$A_N = (f_{12} + \mathrm{i}f_{11})B_1 \quad \text{and} \quad B_N = (f_{22} + \mathrm{i}f_{21})B_1. \tag{7}$$

Equating A_N and $-B_N$ from (7), we obtain an eigenvalue equation for the propagation constant β, i.e. $F(\beta) = 0$. In general, the propagation constant can be expressed as $\beta = \beta_\mathrm{r} + \mathrm{i}\beta_\mathrm{i}$ with β_r being the real part and β_i the imaginary part. A plot of $1/|F|^2$ with β shows a number of Lorentzian-shaped resonance peaks, each of which corresponds to a mode. The value of β corresponding to the resonance peak gives the real part of the propagation constant β_r and the FWHM of the Lorentzian gives the imaginary part β_i. In this way, both the real part and the imaginary part of β can be calculated. The effective indices of modes can be calculated by the real part of the propagation constant, while the leakage losses of the modes can be estimated by the imaginary part.

The SM operation of the structure can be ensured by a high differential leakage loss between the first two modes and a nominal loss to the fundamental mode. Bending sensitivity of the structure can be estimated by representing the bent waveguide by a straight waveguide having an effective refractive index profile in a transformed coordinate $\xi = \sqrt{x^2 + y^2} - \rho$, where ρ is the bending radius, as mentioned in detail in Ref. [21].

3 Results and discussion

We have carried out numerical simulation for the following parameters unless stated otherwise, which are typical for silica on silicon waveguides:

$$n_1 = 1.462, \quad n_2 = 1.442, \quad a = 10\ \mu\mathrm{m}, \quad b = 16\ \mu\mathrm{m}, \quad d = 1.5\ \mu\mathrm{m}, \quad \Lambda = 4.5\ \mu\mathrm{m}, \quad \lambda = 1.55\ \mu\mathrm{m}. \tag{8}$$

The waveguides can be fabricated by depositing silica and fluorine-doped silica layers of different refractive indices on silicon wafers by using a Helicon diffusion plasma reactor. The refractive indices of the depressed layers can be controlled by varying the level of fluorine doping achieved through passing a small amount of CF_4 into the plasma [26].

3.1 Single-mode operation

A high differential leakage loss between the fundamental and higher-order modes form the criterion for the SM behavior of the waveguide. The leakage loss of the modes can be controlled by the cladding profile, characterized by the profile shape parameter q. To investigate the effect of cladding profile on the leakage loss, we have plotted its variation as a function of q for the first few modes of the waveguide as shown in Fig. 2a. According to (1), $q = 0$ corresponds to the structure where all the depressed cladding layers have the same refractive index n_2 and $q = \infty$ corresponds to a waveguide with only one index dip in the cladding, which is a conventional leaky waveguide. For $q = 0$, the first higher-order mode TE_1 has $\sim$1 dB/mm loss and it would require a $\sim$2-cm-long waveguide to strip it off by inserting 20 dB loss. A waveguide with $q = 0$ would therefore not be interesting for SM operation. It is clear from the figure that the leakage losses of the modes increase with q and eventually approach the values corresponding to the losses of a conventional leaky waveguide. The differential leakage loss between the modes also, in general, increases with q. An interesting feature of the leakage loss curve of the TE_1 mode is a peak around $q = 0.75$, which suggests a resonant coupling of the TE_1 mode to one of the highly lossy modes of the high-index cladding layer. This resonant coupling significantly enhances the differential leakage loss between the TE_0 and TE_1 modes in the structure. A waveguide that introduces a sufficiently high leakage loss to the TE_1 mode (>5 dB/mm) and a nominal loss to the fundamental mode TE_0 (<0.5 dB/mm) would be appropriate for effective SM operation. Figure 2a shows that for the parameters given

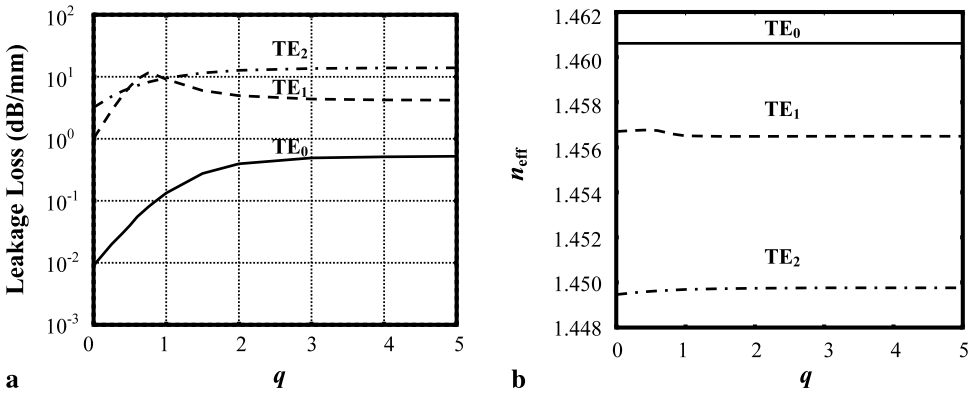

Fig. 2 Effects of the profile parameter q on (**a**) the leakage losses and (**b**) the effective indices of TE_0, TE_1, and TE_2 modes of the waveguide

by (8), a structure with $0.5 < q < 2.0$ meets the criterion for effective SM operation. As an example, for $q = 1$ the TE_1 mode suffers from ~9 dB/mm loss and can be stripped off from the waveguide in a propagation through 2 mm in the waveguide, while the TE_0 mode suffers from a nominal loss of 0.26 dB over the same distance. Thus, the waveguide is effectively SM with core width of 10 μm and NA = 0.24. For SM operation, the proposed design offers a core width three times larger than that of the conventional waveguide having the same NA. We have also investigated the effect of q on the effective indices of modes as shown in Fig. 2b. We see that the effective index of the TE_0 mode remains unperturbed with variations in q. The TE_1 mode shows a slight variation in effective index for the values of q between 0 and 1, indicating the perturbations due to high-index cladding layers.

3.2 Modal field

The modal fields of the TE_0 and TE_1 modes are shown in Fig. 3a. One can see the oscillations in the cladding region that indicate the leakage of energy from core to cladding for both the modes. The larger amplitude of oscillations indicates higher leakage loss for the TE_1 mode. The contour plot of the TE_0 mode clearly indicates that most of the power is well confined inside the guiding core. The 1/e mode size of the fundamental mode is 7 μm and is indicated by the dashed lines in Fig. 3b.

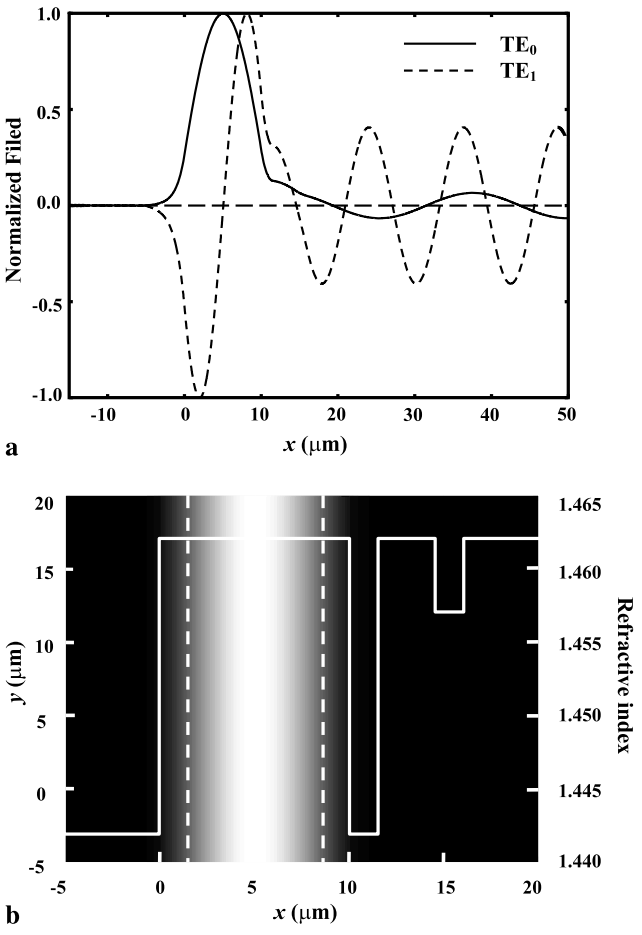

Fig. 3 (**a**) Normalized modal field plots of TE_0 and TE_1 modes at 1.55-μm wavelength for $q = 1$. (**b**) Contour plot of fundamental mode along with profile. The *dashed lines* indicate 1/e mode-size boundaries

3.3 Effects of cladding parameters

Apart from the profile parameter q, the normalized depressed layer width d/Λ and the cladding width $b-a$ are the other cladding parameters that affect the absolute and differential leakage losses of the modes and hence the single-mode behavior of the waveguide. Figure 4 shows the effect of normalized cladding width b/Λ on the leakage loss of the modes for $q = 1.5$. The leakage loss of the TE_1 mode is about 7.25 dB/mm with a ripple of ±1.25 dB/mm, which is a signature of coupling to the high-index cladding layer. The loss of the TE_0 mode decreases with b/Λ and eventually settles down to a value less than 0.0002 dB/mm for $b/\Lambda > 8$. An increase in b/Λ results in a greater number of depressed layers in the cladding region, which improves the confinement of the modes. The high differential leakage loss for larger values of b/Λ is due to the fact that the refractive index of the depressed cladding layers farther from the core is smaller than the effective index of the TE_0 mode but larger than that of the TE_1 mode. The maximum possible value of b is limited by fabrication constraints. A practical value of b may accommodate five depressed cladding layers, with which one can bring down the leakage loss of the TE_0 mode to below 0.002 dB/mm and the TE_1 mode can be leaked out in 2.5-mm propagation distance.

The effect of the width of depressed cladding layers on SM behavior of the waveguide is shown in Fig. 5, where we have plotted the variation of leakage loss as a function

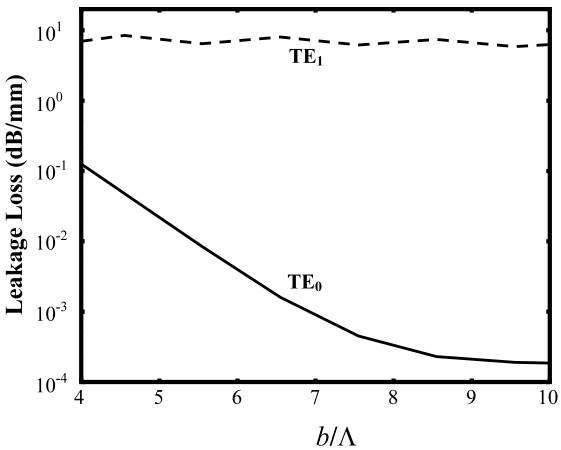

Fig. 4 Variations of leakage losses of TE_0 and TE_1 modes as a function of normalized cladding width b/Λ for profile parameter $q = 1.5$

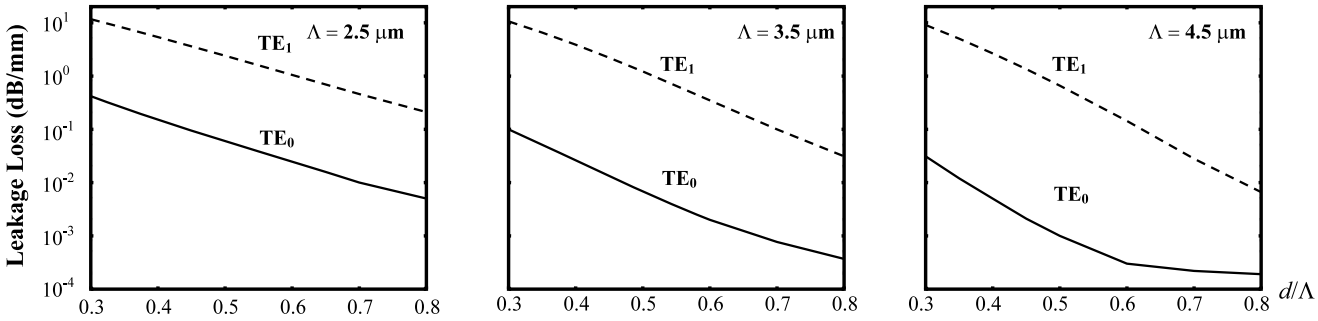

Fig. 5 Variations of leakage losses of TE_0 and TE_1 modes as a function of normalized depressed cladding width d/Λ for profile parameter $q = 1.5$ and three different values of Λ (2.5, 3.5, and 4.5 μm)

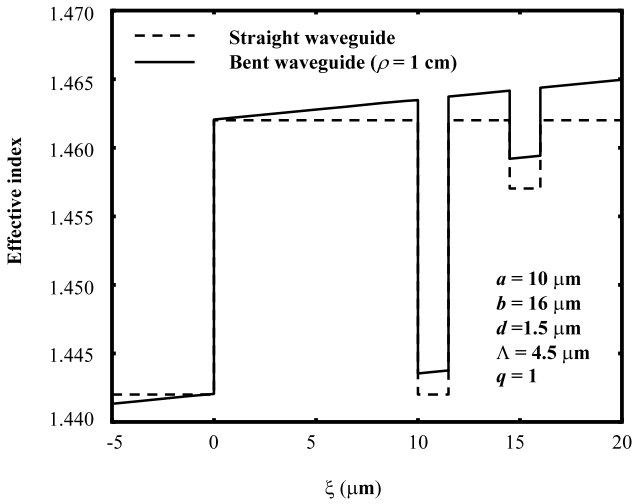

Fig. 6 Effective refractive index profile of a bent waveguide corresponding to the bend radius $\rho = 1$ cm

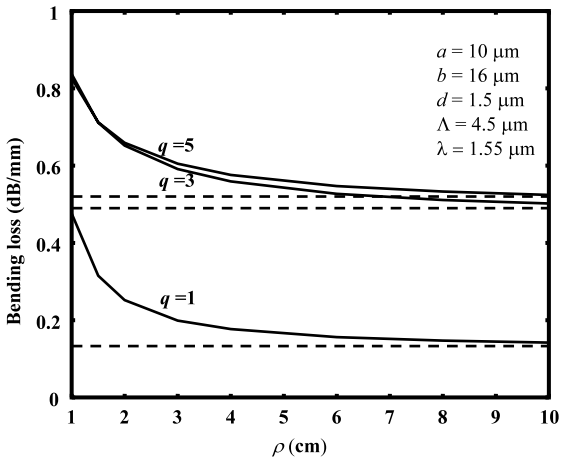

Fig. 7 Variation of the bending loss of the multi-clad leaky waveguide with bend radius for $q = 1$, 3, and 5. The *dashed lines* represent the values of the leakage losses for the corresponding straight waveguides

of d/Λ for three different values of Λ. We can see from the figure that for a given Λ, an increase in d/Λ improves the confinement of the modes. However, a larger value of Λ leads to higher differential leakage loss. For a given value of Λ, increase in d/Λ increases the width of the depressed cladding layers, which results in lower leakage losses for the modes. For a given value of d/Λ, an increase in Λ increases the width of both the depressed and the high-index cladding layers. This improves the confinement of TE_0 and TE_1 modes in different proportions and results in high differential leakage loss as shown in Fig. 5.

3.4 Bending loss

To calculate the bending loss of the waveguide we have replaced the bent waveguide by a straight waveguide with an effective refractive index profile by using a conformal transformation as shown in Fig. 6 for bending radius $\rho = 1$ cm. The bent profile can be analyzed with the help of the TMM to calculate the leakage loss. This approach of calculating bending loss is accurate for bend radii much larger than the guiding core width. We have plotted the variation of bending loss of the TE_0 mode as a function of bending radius for three different values of q as shown in Fig. 7. The results show that the bending loss decreases with the increase in bend radius and settles down to the value corresponding to the leakage loss of the straight waveguide, which is indicated by the dashed line. The waveguide is more sensitive to bending for larger values of q. For all the profiles shown in Fig. 7, the waveguide is relatively insensitive to bending for bending radii larger than 3 cm. As the bending introduces large losses to higher-order modes, it actually helps in stripping off the TE_1 mode.

3.5 A simplified resonant waveguide design

We have noticed in Fig. 2a of Sect. 3.1 that at a particular value of q, the leakage loss of the TE_1 mode shows a peak, leading to high differential leakage loss between the first two modes. The occurrence of the peak was attributed to the resonant coupling of energy from the TE_1 mode to one of the modes supported by the high-index cladding layer. In

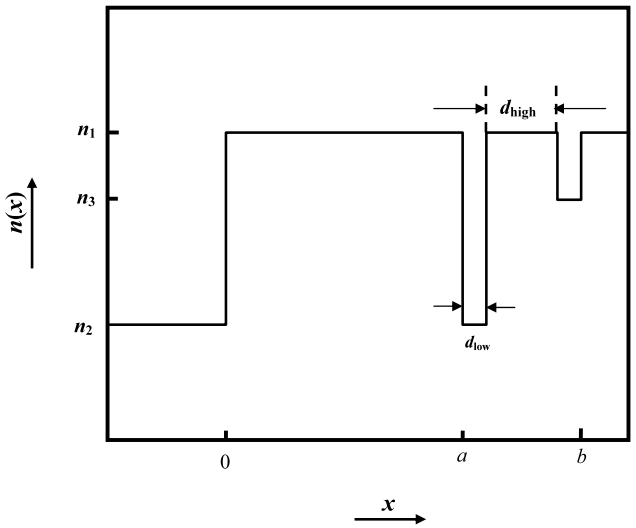

Fig. 8 Refractive-index profile of a resonant multi-clad planar waveguide

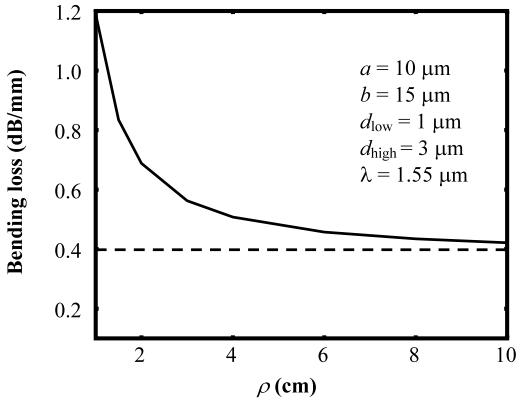

Fig. 9 Bending sensitivity of the multi-clad resonant planar waveguide

this section we utilize this observation to present a simplified leaky design having only two depressed cladding layers, where the differential leakage loss between the modes is optimized to enable an efficient SM leaky structure. The refractive-index profile of the structure is shown in Fig. 8. The cladding of the structure is characterized by two depressed cladding layers each of width d_{low} and refractive indices n_2 and n_3 and one high-index cladding of width d_{high} and refractive index n_1. The width of the cladding can be expressed as $b - a = 2d_{\text{low}} + d_{\text{high}}$. It is assumed that beyond $x = b$ there is an infinitely extended high index region of refractive index n_1. We have carried out calculations for the effective indices and leakage losses of the first few modes for the parameters $n_1 = 1.462$, $n_2 = 1.442$, $n_3 = 1.455$, $a = 10$ μm, $d_{\text{low}} = 1$ μm, $d_{\text{high}} = 3$ μm, $b = 15$ μm, and $\lambda = 1.55$ μm. The waveguide introduces 0.39 dB/mm loss to the TE_0 mode and the loss of the TE_1 mode can be made so high that it becomes comparable to the loss of the TE_2 mode. The actual values of losses of the TE_1 and TE_2 modes are 20.65 and 19.32 dB/mm, respectively. Clearly, the differential leakage loss between the first and the higher-order modes increases significantly. In fact, in this example the SM behavior of the structure is governed by the leakage loss of the TE_2 mode, which would be leaked out after suffering 20 dB loss through 1-mm propagation in the waveguide and the TE_0 mode would suffer from only 0.39 dB loss in this distance. This simplified design based on resonant leakage loss is more promising for efficient SM operation and should be easier to fabricate, too. The bending loss of the resonant waveguide is shown in Fig. 9, which again shows relatively less bending sensitivity of the structure for bending radii larger than 3 cm.

4 Conclusions

We proposed a multi-clad planar waveguide for large-core-area single-mode operation. The waveguide is characterized by a uniform substrate, a uniform core, and a multi-layer cladding having alternate low- and high-index layers. The waveguide has been analyzed by using the TMM to calculate the leakage losses and effective indices of the first few modes. We have carried out a design study of the waveguide for obtaining high differential leakage loss between the first two modes to ensure effective SM operation. A resonant coupling between the TE_1 mode and one of the modes of the high-index cladding layer can lead to significantly high differential leakage loss and an efficient SM operation. We show that the structure with core thickness as large as 10 μm and numerical aperture 0.24 can exhibit SM operation at 1.55-μm wavelength. A waveguide with such a large core is capable of suppressing nonlinear effects and is expected to find applications in the design of high-power waveguide lasers and amplifiers.

References

1. J.I. Mackenzie, IEEE J. Sel. Top. Quantum Electron. **13**, 626 (2007)
2. J.M. Eggleston, T.J. Kane, K. Kuhn, J. Unternahrer, R.L. Byer, IEEE J. Quantum Electron. **20**, 289 (1984)
3. C.L. Bonner, C.T.A. Brown, D.P. Shepherd, W.A. Clarkson, A.C. Tropper, D.C. Hanna, B. Ferrand, Opt. Lett. **23**, 942 (1998)
4. J.N. Walpole, J.P. Donnelly, P.J. Taylor, L.J. Missaggia, C.T. Harris, R.J. Bailey, A. Napoleone, S.H. Groves, S.R. Chin, R. Huang, J. Plant, IEEE Photon. Technol. Lett. **14**, 756 (2002)
5. C. Zmudzinski, D. Botez, L.J. Mawst, A. Bhattacharya, M. Nesnidal, R.F. Nabiev, IEEE J. Sel. Top. Quantum Electron. **1**, 129 (1995)
6. D.P. Shepherd, S.J. Hettrick, C. Li, J.I. Mackenzie, R.J. Beach, S.C. Mitchell, H.E. Meissner, J. Phys. D: Appl. Phys. **34**, 2420 (2001)
7. R.K. Huang, L.J. Missaggia, J.P. Donnelly, C.T. Harris, G.W. Turner, IEEE Photon. Technol. Lett. **17**, 959 (2005)

8. N.G.R. Broderick, D.J. Richardson, D. Taverner, J.E. Caplen, L. Dong, M. Ibsen, Opt. Lett. **24**, 566 (1999)
9. N.G.R. Broderick, H.L. Offerhause, D.J. Richardson, R.A. Sammut, J. Caplen, L. Dong, Opt. Fiber Technol. **5**, 185 (1999)
10. H.L. Offerhaus, N.G. Broderick, D.J. Richardson, R. Sammut, J. Caplen, L. Dong, Opt. Lett. **23**, 1683 (1998)
11. N.G.R. Broderick, H.L. Offerhaus, D.J. Richardson, R.A. Sammut, IEEE Photon. Technol. Lett. **10**, 1718 (1998)
12. Y. Jeong, J.K. Sahu, D.N. Payne, J. Nilsson, Opt. Express **12**, 6088 (2004)
13. Y. Jeong, J.K. Sahu, D.N. Payne, J. Nilsson, Electron. Lett. **40**, 1527 (2004)
14. M. Laroche, P. Jander, W.A. Clarkson, J.K. Sahu, J. Nilsson, Y. Jeong, Electron. Lett. **40**, 855 (2004)
15. J.C. Knight, T.A. Birks, R.F. Cregan, P.St.J. Russell, J.P. De Sandro, Electron. Lett. **34**, 1347 (1998)
16. V. Rastogi, K.S. Chiang, J. Opt. Soc. Am. B **21**, 258 (2004)
17. V. Rastogi, K.S. Chiang, Opt. Lett. **26**, 491 (2001)
18. A. Millo, I. Naeh, Y. Lavi, A. Katzir, Appl. Phys. Lett. **88**, 251101 (2006)
19. V. Rastogi, K.S. Chiang, Electron. Lett. **39**, 1110 (2003)
20. A. Kumar, V. Rastogi, J. Opt. A **10**, 015303 (2008)
21. A. Kumar, V. Rastogi, K.S. Chiang, Appl. Phys. B **85**, 11 (2006)
22. A. Kumar, V. Rastogi, K.S. Chiang, Appl. Phys. B **90**, 507 (2008)
23. M.R. Ramadas, E. Garmire, A.K. Ghatak, K. Thyagarajan, M.R. Shenoy, Opt. Lett. **14**, 376 (1989)
24. M.R. Ramadas, R.K. Varshney, K. Thyagarajan, A.K. Ghatak, J. Lightwave Technol. **7**, 1901 (1989)
25. K. Wörhoff, P.V. Lambeck, A. Driessen, J. Lightwave Technol. **17**, 1401 (1999)
26. D.R. Beltrami, J.D. Love, A. Durandet, A. Samoc, M. Samoc, B. Luther-Davies, R.W. Boswell, Electron. Lett. **32**, 549 (1996)